

Gas-Particle Partitioning of PCBs and PAHs in the Chicago Urban and Adjacent Coastal Atmosphere: States of Equilibrium

MATT F. SIMCIK, THOMAS P. FRANZ, HUIXIANG ZHANG, AND STEVEN J. EISENREICH*

Department of Environmental Sciences, Rutgers, The State University of New Jersey, College Farm Road, New Brunswick, New Jersey 08903

Simultaneous air samples were taken in Chicago and over southern Lake Michigan as part of the AEOLUS Project (Atmospheric Exchange Over Lakes and Oceans). Gas and particle phase concentrations of polychlorinated biphenyls (PCBs), polycyclic aromatic hydrocarbons (PAHs), and total suspended particles (TSP) were measured over 12 h periods during July, 1994, and January, 1995. Partitioning of PCBs and PAHs between gas and particle phases was well correlated with the subcooled liquid vapor pressure (p_L^o) for individual samples, but the relationship differed among samples. For all but a few of the samples the slopes of the $\log K_p$ vs $\log p_L^o$ lines were statistically greater than -1 . Other investigators who have found similar results have concluded that the PCBs/PAHs were not at equilibrium; however, other factors indicate that the PCBs and PAHs in the Chicago/Lake Michigan atmosphere are at equilibrium. Slopes of the regressions of $\log K_p$ vs $\log p_L^o$ from samples of continental background origin, and therefore assumed to have had sufficient atmospheric residence times to reach equilibrium, are among the shallowest measured (-0.70 to -0.53 and -0.16 to -0.56 for PAHs and PCBs, respectively). One pair of samples where the air mass is believed to have been sampled twice, once in the urban area and again ~ 3.4 h downwind, shows no difference in partitioning. PCBs and PAHs measured in Chicago and over Lake Michigan were apparently at equilibrium between the gas and particle phases. A slope of -1 in the regression of $\log K_p$ vs $\log p_L^o$ is not necessary to describe equilibrium partitioning. Differences in particulate matter may be responsible for the shallow slopes observed.

Introduction

The partitioning of semivolatile organic compounds (SOCs) in the atmosphere is an important factor in their fate, transport, and transformation in urban and adjacent coastal atmospheres. The partitioning of SOC between the gas and particulate phases is described as either surface adsorption (1) or absorption into organic matter (2). Both paradigms relate the total suspended particulate matter (TSP in micrograms per cubic meter), normalized partition coefficient, K_p , to the subcooled liquid vapor pressure, p_L^o . K_p is defined as $(F/TSP)/A$, where F and A are the filter and adsorbent

retained SOC concentrations (ng/m^3), respectively. The relationship for physical adsorption is (1):

$$K_p = \frac{(F/TSP)}{A} = \frac{N_s a_{TSP} T e^{(Q_d - Q_v)/RT}}{2133 p_L^o} \quad (1)$$

where K_p ($\text{m}^3/\mu\text{g}$) is the partition coefficient, N_s is the surface area concentration of adsorption sites (mol/cm^2), a_{TSP} is the surface area of the TSP ($\text{cm}^2/\mu\text{g}$), T is the temperature (K), R is the molar gas constant ($8.314 \times 10^{-3} \text{ kJ K}^{-1} \text{ mol}^{-1}$), Q_d and Q_v are the enthalpies of desorption (kJ/mol) and volatilization, respectively, and p_L^o is the subcooled liquid vapor pressure (Pa). The constant in eq 1 differs from that of eq 44 of Pankow (1) because of the use of Pascals for the subcooled liquid vapor pressure instead of Torr. The relationship describing K_p for absorptive partitioning is as follows (2):

$$K_p = \frac{(F/TSP)}{A} = \frac{f_{om} 760 RT}{MW_{om} \gamma p_L^o 10^6} \quad (2)$$

where f_{om} is the fraction of organic matter on the TSP, MW_{om} is the molecular weight of the organic matter, and γ is the activity coefficient of the adsorbate in the organic matter. Both eqs 1 and 2 lead to a linear relationship between $\log K_p$ and $\log p_L^o$:

$$\log K_p = m_r \log p_L^o + b_r \quad (3)$$

At equilibrium, the slope for either adsorption or absorption should be near -1 given the following assumptions: for adsorption, the difference between the enthalpies of desorption and volatilization and the number of available adsorption sites must remain constant over a compound class (1); for absorption the activity coefficients must remain constant over a compound class (2). The difference between the enthalpies of desorption and volatilization is expected to remain constant over a compound class (3), but it is not necessarily true for all types of atmospheric particles even under similar atmospheric conditions (4). Testing the validity of the assumption made for absorption is accomplished using the relationship between octanol-air partition coefficients (K_{OA}) and p_L^o . Octanol-air partition coefficients may reflect the equilibrium partitioning between air and an organic matrix at a specific temperature, and are defined as the concentration of SOC in octanol (mass SOC/volume octanol) over the concentration of SOC in air (mass SOC/volume air) (5). Harner and Bidleman (6) reported K_{OA} values for multiortho and non/monoortho PCBs and found that plots of $\log K_{OA}$ vs $\log p_L^o$ yielded slopes of -1.015 and -1.268 for multi- and non/monoortho PCBs, respectively at 20°C . Therefore, the assumption of constant activity coefficient in octanol seems to hold true for multiortho PCBs, but not for non/monoortho PCBs. Plots of $\log K_{OA}$ vs $\log p_L^o$ for PAHs also yielded slopes very near -1 (7). Therefore, if octanol is an appropriate surrogate for atmospheric organic matter, equilibrium absorptive partitioning for multiortho PCBs and PAHs should yield slopes near -1 for the relationship of $\log K_p$ vs $\log p_L^o$. Despite the theoretical basis for this relationship and some field and lab results (1, 8–12), many field measurements yield slopes shallower than -1 (11, 13–16).

* Author to whom correspondence should be addressed. E-mail: eisenreich@aesop.rutgers.edu.

This study is part of the larger AEOLUS Project (Atmospheric Exchange Over Lakes and Oceans), whose hypothesis is that emissions of PCBs and PAHs into the coastal urban atmosphere enhance atmospheric depositional fluxes to adjacent great waters such as Lake Michigan off Chicago, IL/Gary, IN, and Chesapeake Bay off Baltimore, MD. The urban air emissions in Chicago increase the adjacent coastal atmospheric PCB and PAH concentrations by factors of 4 and 12, respectively (17). Gas-particle partitioning is an important factor in determining the mode of deposition (i.e., air-water exchange, dry and wet deposition). This study represents the largest data set of gas and particulate phase SOCs, temperature, relative humidity, and TSP assessed simultaneously in an urban and coastal environment. The data set offers a unique perspective into the question of equilibrium partitioning of PCBs and PAHs in the urban and adjacent coastal atmospheres. In particular we question the necessity for $\log K_p$ vs $\log p_i^0$ plots to produce slopes of -1 when PCBs and PAHs are at equilibrium between the gas and particle phases.

Experimental Methods

The sampling scheme and experimental methods for PCBs and PAHs are described elsewhere (17). In general, air samples were taken simultaneously at an urban location in south Chicago, IL, and over Lake Michigan aboard the *RV Lake Guardian* during May and July, 1994, and January, 1995. The high volume air samplers were equipped with glass fiber filters (GFFs) to collect particulate phase compounds and polyurethane foam plugs (PUF) to collect the gas phase compounds. As reported in Simcik et al. (17), all of the PAHs and PCBs were corrected for field blanks. Of the 27 PAHs analyzed by gas chromatography/mass spectrometry, only the eleven for which vapor pressure vs temperature relationships are available were used in this study. All of the 80 PCB congener peaks, analyzed by gas chromatography with electron capture detection, were used in this study. Two 12 h samples were collected each day (8:00 am–8:00 pm and 8:00 pm–8:00 am) to minimize effects of changing temperature and atmospheric concentrations of the PCBs, PAHs, and TSP. Total suspended particulate matter was determined during July and January using an Anderson Dichotomous sampler dividing the TSP into two size ranges (>2.5 and <2.5 μm), collected on Teflon filters and analyzed gravimetrically. Temperature, wind direction, speed, and relative humidity were collected with meteorological towers at both sites and the data stored on computer.

Suitability of Data Set. Before an investigation into the states of equilibria can be attempted, the relationship of the measured PCB and PAH concentrations on GFF and PUF to the true gaseous and particulate concentrations must be assessed. Sampling artifacts associated with the GFF and PUF can affect the apparent gas-particle distributions of SOCs. The GFF may exhibit two such artifacts with counteracting effects on the distribution. Gaseous PCBs or PAHs may sorb to the filter surface and particles collected on the filter (18–20). Second, the more volatile compounds may be stripped from the filter by continuing gas flow if the gas phase concentration decreases or the temperature increases over the sampling period (10, 21–24). Gas adsorption increases the apparent particle phase concentrations and decreases the apparent gas phase concentration. The extent of gas adsorption is often assessed using a second filter, but interpreting results from this secondary filter is problematic (10). Backup filters were used in 10 samples collected in Chicago and over Lake Michigan. The percent mass on secondary filters (avg \pm sd) for PAHs are as follows: fluorene, $3 \pm 5\%$; phenanthrene, $5 \pm 6\%$; anthracene, $3 \pm 4\%$; fluoranthene, $5 \pm 6\%$; pyrene, $4 \pm 5\%$; benz[a]anthracene, $3 \pm 5\%$; chrysene, $3 \pm 4\%$; benzo[b+k]fluoranthene, $2 \pm 3\%$;

benzo[e]pyrene, $3 \pm 3\%$; benzo[a]pyrene, $2 \pm 3\%$; benzo[ghi]perylene, $2 \pm 3\%$. PCBs were not detected on any secondary filter. While adsorption to the secondary filter would cause the greatest change in K_p for the PAHs with fraction on particulate values nearest 0.5 (i.e., PAHs distributed evenly between the two phases), this effect is <0.5 log units. Therefore, the backup filters were neither subtracted from the particle phase concentration nor added to the gas phase concentration. Volatilization from the filter has the opposite affect, and was undeterminable. Breakthrough of volatile PCBs and PAHs from the PUF can also adversely affect K_p (9, 19, 25–27). A split PUF was used on six samples and contaminant mass on the back PUF was compared to the total mass. During July when the ambient temperature was highest, appreciable amounts of only the most volatile PAHs (fluorene through pyrene) were found on the back half of the PUF. The mass on the back half averaged $52 \pm 4\%$ ($n = 6$) of the total mass on PUF for fluorene, but only $7 \pm 7\%$ ($n = 6$) for phenanthrene, and much less for the other PAHs. Individual PCBs on the back PUFs were all less than 15% of their total PUF masses. Because of the evidence against significant sampling artifacts and studies comparing Hi-Vol samplers to a diffusion separator (28), denuder (29), and impactors (28, 30), which showed little difference in the gas-particle partitioning, we conclude that the GFF and PUF associated concentrations of PCBs and PAHs are a good estimate of the true gas and particle phase concentrations in these samples.

Results and Discussion

All meteorological data, TSP, atmospheric PCB and PAH concentrations, and regression statistics are available in the Supporting Information. A summary of the number of samples, analytes used, and average atmospheric concentrations is provided in Table 1. Due to the large number of PCBs analyzed, 55 peaks corresponding to 80 congeners, only the 40 most prominent have been reported in Table 1. TSP concentrations ranged from 11 to 71 $\mu\text{g}/\text{m}^3$ in Chicago and 1.5 to 29 $\mu\text{g}/\text{m}^3$ over Lake Michigan. Twelve hour average temperature and relative humidity values ranged from 277 to 302 K and 56 to 96%, respectively. The temperature-dependent vapor pressures were calculated for all PCB congeners based on Falconer et al. (31), and for 11 PAHs from a compilation of literature data by Liu (28) at the average ambient temperature of the sampling period. Only those PAHs and PCBs that had concentrations above the detection limit for a given sample were used in the $\log K_p$ vs $\log p_i^0$ regressions. Vapor pressures of coeluting PCBs were calculated for the dominant PCB in each peak, the first congener listed. This is justified by the fact that coeluting PCBs have very similar vapor pressures (31).

Regressions of $\log K_p$ vs $\log p_i^0$ for both Chicago and Lake Michigan samples gave high correlations for individual samples for both PAHs ($r^2 = 0.85$ – 0.98) and for most PCBs ($r^2 = 0.10$ – 0.71), but the slopes and intercepts amongst samples varied greatly (Figures 1–4). Five of the PCB samples over Lake Michigan exhibited no relationship with vapor pressure (i.e., Figure 4c). These samples were omitted from Figure 4d. These samples were ones in which the wind direction was from the north bringing very low concentrations of PCBs. In addition, the particle phase accounted for less than 1% of the total PCB. Because of this, it is impossible to draw conclusions from such samples. For all PCBs at the Chicago and Lake Michigan sites and all but seven of the PAH comparisons for Chicago and three for Lake Michigan, the 95% confidence intervals about the regressed slopes exclude the value of -1 . When all of the data for PAH partitioning in Chicago are regressed, the slope (-0.64) and intercept (-3.47 ; $r^2 = 0.78$) compare well with results by Cotham and Bidleman (16) for similar PAHs from Chicago

TABLE 1. Summary of Average Concentrations, Analytes, and Number of Samples^a

analyte	Chicago July southwest winds					Chicago July north winds					Chicago January					Lake Michigan July southwest winds					Lake Michigan July north winds				
	avg conc	std dev	avg % particle	std dev	N	avg conc	std dev	avg % particle	std dev	N	avg conc	std dev	avg % particle	std dev	N	avg conc	std dev	avg % particle	std dev	N	avg	std dev	avg % particle	std dev	N
fluorene	18.1	11.5	1.5%	2.6%	10	17.4	10.1	2%	2%	8	7.8	2.8	10%	6%	4	8.2	4.9	0.4%	0.3%	10	2.10	1.68	0.4%	0.4%	5
phenanthrene	98.4	55.7	1.5%	1.9%	10	65.8	32.1	4%	3%	8	21.2	10.8	24%	10%	4	18.2	9.8	1.1%	0.8%	10	4.01	3.96	2.3%	2.0%	5
anthracene	10.6	9.3	2.3%	2.3%	10	5.7	3.0	7%	5%	8	3.2	2.4	28%	9%	4	0.7	0.6	4.9%	4.0%	10	0.14	0.13	8.9%	11.8%	4
fluoranthene	28.1	17.0	11%	11%	10	14.7	8.2	22%	12%	8	12.9	9.6	55%	8%	4	5.1	2.9	6.4%	3.9%	10	1.06	0.99	13%	10%	5
pyrene	16.2	12.4	14%	14%	10	10.1	6.8	26%	12%	8	10.9	8.1	54%	8%	4	3.1	2.2	10%	7%	10	0.47	0.42	18%	13%	5
benz[a]anthracene	3.1	5.6	73%	19%	10	1.8	1.9	89%	7%	7	5.2	5.0	95%	4%	2	0.5	0.4	44%	14%	7	0.05	0.03	53%	10%	3
chrysene	3.8	5.7	66%	17%	10	2.0	1.8	77%	12%	7	6.0	6.1	92%	6%	2	1.4	0.8	26%	8%	7	0.05	0.03	53%	10%	3
benzo[b+k]fluoranthene	12.1	17.7	89%	11%	3	2.9	NA	96%	NA	1	2.8	NA	94%	NA	1	1.2	1.1	79%	12%	10	0.09	0.10	75%	13%	5
benzo[e]pyrene	7.4	9.4	91%	10%	2	NA	NA	NA	NA	0	1.2	NA	95%	NA	1	0.5	0.5	86%	8%	10	0.07	0.09	81%	12%	5
benzo[a]pyrene	0.5	NA	89%	NA	1	NA	NA	NA	NA	0	1.5	NA	94%	NA	1	0.3	0.2	94%	7%	8	0.07	0.10	91%	8%	4
benzo[ghi]perylene	0.7	0.3	91%	8%	3	2.7	1.1	99%	0%	2	1.4	NA	96%	NA	1	1.2	NA	88%	NA	1	0.24	NA	96%	NA	1
PCB-4+10	59.2	33.2	1.7%	2.8%	9	63.9	31.9	5.0%	10.3%	6	NA	NA	NA	NA	0	117.4	29.3	0.3%	0.2%	6	54.2	NA	0.9%	NA	1
PCB-6	66.3	47.4	0.65	0.6%	9	62.1	87.1	1.0%	1.1%	6	10.9	4.4	5.6%	1.9%	2	8.3	3.3	2.9%	4.8%	9	3.8	5.0	2.2%	1.2%	5
PCB-18	288.6	236.2	0.8%	0.8%	9	127.4	93.1	0.4%	0.4%	6	NA	NA	NA	NA	0	52.2	8.7	0.9%	1.0%	9	25.3	14.4	0.9%	0.9%	6
PCB-24+27	54.4	34.4	0.7%	0.5%	9	21.7	18.0	1.4%	0.8%	6	8.9	5.3	4.3%	1.0%	2	11.8	3.3	1.4%	1.1%	8	6.3	0.6	0.6%	0.9%	2
PCB-16+32	312.2	257.0	0.8%	0.8%	9	127.2	100.2	1.4%	0.4%	6	8.9	5.3	4.3%	1.0%	2	55.0	10.8	0.6%	0.5%	10	23.6	16.4	2.5%	2.1%	6
PCB-26	71.8	72.5	1.4%	0.7%	8	32.2	19.8	2.1%	0.9%	5	NA	NA	NA	NA	0	11.8	2.5	0.8%	0.6%	7	6.1	0.0	1.2%	0.4%	2
PCB-25	30.7	27.7	1.7%	1.6%	9	16.5	10.5	3.1%	2.2%	5	5.6	NA	1.4%	NA	1	6.7	1.3	4.5%	3.9%	8	1.5	1.9	9.4%	6.9%	4
PCB-31+28	649.9	572.9	1.1%	1.0%	9	258.3	170.4	1.4%	0.7%	6	72.8	31.8	2.9%	0.6%	2	101.2	20.4	0.2%	0.2%	10	71.3	10.6	0.7%	0.7%	3
PCB-21+33+53	347.4	422.1	1.0%	0.8%	9	108.7	81.6	1.4%	0.6%	6	233.1	88.3	0.8%	0.4%	2	34.8	8.4	0.5%	0.3%	10	16.7	12.5	0.8%	0.6%	6
PCB-45	38.2	33.5	1.5%	2.4%	8	32.0	19.0	1.4%	0.2%	2	NA	NA	NA	NA	0	13.8	3.9	0.7%	0.8%	6	4.5	NA	0.4%	NA	1
PCB-52+43	132.0	95.9	1.4%	1.1%	9	68.5	27.9	1.4%	0.8%	6	20.3	1.8	8.2%	2.6%	2	37.7	7.4	0.5%	0.4%	9	14.8	7.9	0.5%	0.6%	6
PCB-49	110.4	85.7	1.0%	0.8%	9	52.0	20.7	2.0%	1.0%	6	11.0	NA	15.1%	NA	1	29.3	5.5	0.5%	0.4%	9	9.6	8.2	0.5%	0.9%	2
PCB-47+48	78.9	76.6	3.7%	3.2%	9	41.2	21.3	13.9%	11.3%	6	46.9	55.6	51.4%	60.5%	2	12.5	5.0	19%	14%	7	24.6	7.6	9.1%	3.0%	2
PCB-44	180.4	126.8	1.4%	1.1%	9	82.8	37.9	1.4%	0.9%	6	15.7	4.1	10.9%	3.1%	2	40.5	9.9	0.7%	2.0%	9	12.8	8.5	1.0%	1.0%	7
PCB-37+42	152.1	103.6	1.0%	1.1%	9	54.7	37.0	1.5%	0.9%	6	12.3	1.2	2.6%	0.3%	2	28.7	6.8	0.5%	0.4%	7	7.5	5.3	3.5%	3.6%	6
PCB-41+71+64	161.1	162.2	1.2%	1.2%	9	67.3	37.5	1.3%	1.3%	6	15.8	2.4	5.6%	1.1%	2	33.1	7.8	0.7%	0.6%	8	10.4	6.9	2.1%	2.6%	6
PCB-74	58.7	61.0	2.6%	2.2%	9	50.0	4.1	2.2%	1.1%	2	6.4	16.0%	NA	1	30.9	17.4	2.3%	3.0%	4	NA	NA	NA	NA	0	
PCB-70+76	151.6	112.3	2.6%	1.8%	9	83.0	29.5	3.6%	1.7%	6	22.6	1.1	20.5%	3.9%	2	33.5	6.5	1.3%	0.8%	10	15.3	10.2	1.3%	0.9%	7
PCB-66+95	452.9	776.9	1.3%	0.7%	9	111.2	41.8	2.8%	3.7%	6	14.9	0.7	31.3%	13.5%	2	29.3	18.4	1.3%	1.4%	9	29.1	16.5	0.3%	0.4%	5
PCB-56+60	103.8	123.3	2.3%	1.4%	9	49.9	20.5	2.6%	2.2%	6	7.4	0.8	21.9%	6.6%	2	22.4	5.0	0.6%	0.3%	9	6.5	5.6	5.9%	8.6%	3
PCB-101	69.6	36.6	2.3%	1.5%	9	36.9	9.6	3.1%	1.4%	6	11.2	2.8	27.7%	14.3%	2	17.7	3.3	1.1%	0.5%	10	8.3	4.7	2.2%	1.8%	6
PCB-97	28.6	17.3	2.8%	1.5%	9	14.9	4.2	4.8%	2.9%	6	4.1	0.6	42.4%	8.7%	2	7.7	1.4	1.9%	2.7%	8	3.9	1.8	1.0	0.6%	4
PCB-87+81	38.4	24.3	4.2%	2.0%	9	18.7	3.8	9.7%	4.2%	6	8.3	2.4	45.0%	12.2%	2	10.7	2.8	2.8%	2.0%	4	NA	NA	NA	NA	0
PCB-110+77	127.2	75.9	3.4%	2.0%	9	57.9	14.8	5.1%	3.2%	6	16.1	3.5	41.9%	5.5%	2	25.7	5.4	1.2%	0.5%	10	14.0	9.0	1.0%	0.6%	6
PCB-151	14.5	5.5	3.7%	2.1%	9	7.4	2.0	5.1%	3.9%	5	1.8	0.3	31.2%	7.2%	2	7.8	3.3	1.8%	1.1%	9	3.0	1.2	1.7%	1.6%	6
PCB-149	39.6	20.4	5.3%	2.8%	9	19.9	3.9	6.7%	3.6%	6	5.5	1.6	35.2%	18.8%	2	10.4	2.4	2.0%	2.0%	10	5.0	1.8	1.5%	1.3%	5
PCB-118	50.4	33.5	6.3%	3.75%	9	21.8	4.1	9.9%	7.4%	6	6.8	1.6	50.6%	22.8%	2	10.1	2.0	1.9%	1.2%	9	5.3	2.0	1.9%	1.3%	5
PCB-153+132+105	99.7	59.7	7.1%	4.1%	9	47.0	9.3	10.8%	7.3%	6	16.0	7.4	54.2%	10.4%	2	24.4	5.5	2.2%	1.4%	10	11.9	5.7	1.8%	1.9%	4
PCB-141	9.4	5.8	3.8%	3.2%	9	5.6	2.1	14.8%	16.1%	6	16.0	7.4	54.2%	10.4%	2	24.4	5.5	2.2%	1.4%	10	1.4	2.8%	3.8%	2	
PCB-163+138	61.6	42.9	9.5%	5.3%	9	25.3	5.0	13.9%	9.0%	6	3.8	0.7	20.1%	5.9%	2	13.5	3.4	3.3%	2.5%	10	5.5	3.1	2.6%	2.5%	6
PCB-187+182	10.7	3.0	9.6%	3.3%	9	6.2	1.5	12.2%	8.6%	6	NA	NA	NA	NA	0	4.1	1.1	5.3%	2.5%	10	5.5	3.1	2.6%	2.5%	6
PCB-183	6.3	2.6	9.3%	7.2%	8	3.8	1.2	8.9%	9.4%	6	0.7	0.2	58.5%	2.9%	2	2.7	1.0	5.1%	4.7%	9	0.7	0.4	5.5%	6.0%	7
PCB-174	7.0	3.3	11.5%	7.2%	9	2.9	0.9	14.2%	18.0%	5	0.8	NA	51.3%	NA	1	3.1	1.4	3.9%	3.2%	8	1.3	0.6	2.2%	1.4%	2
PCB-177	4.5	2.1	11.9%	7.6%	9	2.8	1.1	23.7%	15.3%	6	1.6	1.3	85.9%	11.3%	2	1.9	0.7	3.8%	3.1%	8	0.6	0.4	8.0%	5.6%	3
PCB-202+171+156	6.4	1.7	8.9%	5.9%	9	3.7	9.8	14.0%	11.9%	5	0.9	0.4	38.4%	14.7%	2	1.9	0.7	3.8%	3.1%	8	0.6	0.4	8.0%	5.6%	3
PCB-180	53.9	23.0	16.2%	8.2%	9	42.9	9.2	21.2%	12.7%	6	13.4	8.1	49.4%	14.5%	2	8.6	2.7	10%	6%	10	4.1	2.3	5.0%	4.1%	7
PCB-170+190	10.3	8.7	33.8%	19.3%	9	5.8	2.5	36.8%	21.8%	5	4.0	3.5	96.4%	3.6%	2	2.3	1.5	13%	7%	7	1.1	0.6	9.9%	3.1%	6
PCB-201	6.5	2.0	17.0%	7.4%	9	4.6	1.5	31.2%	14.4%	6	1.5	0.0	80.6%	5.9%	2	2.9	0.9	11%	5%	9	0.9	0.5	17.0%	11.2%	7
PCB-203+196	7.7	2.9	18.9%	12.2%	9	4.7	2.1	26.6%	19.5%	6	1.5	NA	83.9%	NA	1	3.3	0.9	11%	10%	9	1.0	0.6	9.8%	5.1%	6
PCB-195+208	5.3	6.6	39.2%	21.2%	9	3.0	1.1	48.9%	16.7%	6	1.1	0.4	87.5%	1.2%	2	1.8	0.9	14%	16%	5	NA	NA	NA	NA	0

^a PAH concentrations in nanograms per cubic meter, PCB concentrations in picograms per cubic meter.

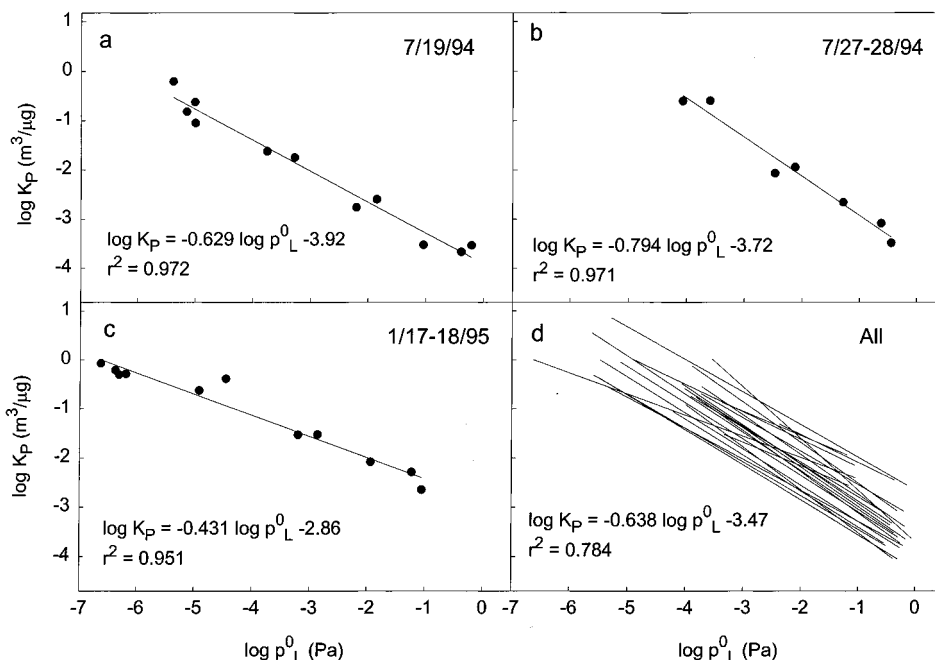


FIGURE 1. $\log K_p$ ($\text{m}^3/\mu\text{g}$) vs $\log p_L^0$ (Pa) for PAHs in Chicago (a) 7/19/94 (b) 7/27–28/94, (c) 1/17–18/95, (d) all samples ($n = 22$).

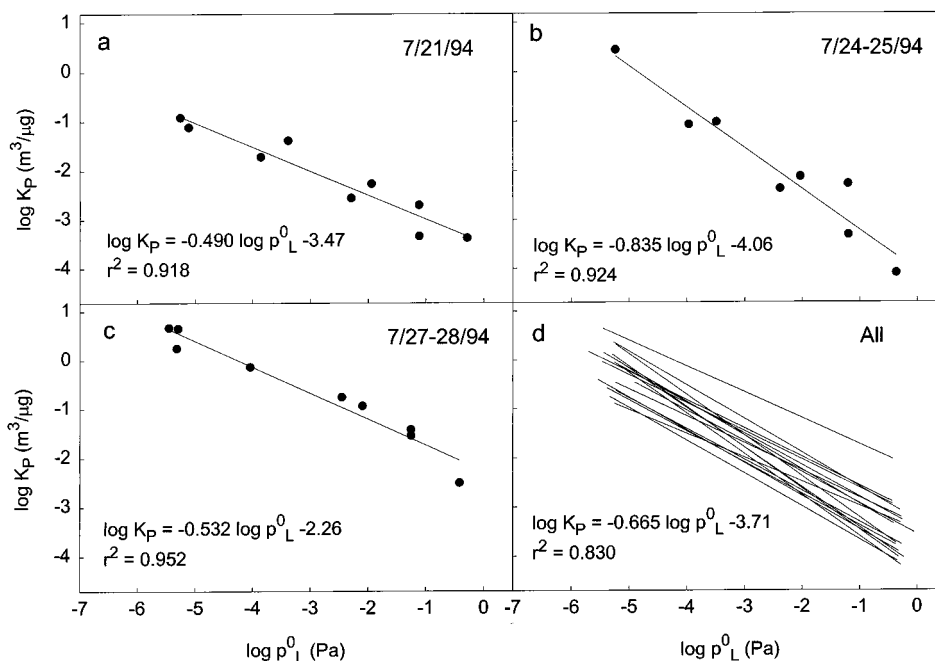


FIGURE 2. $\log K_p$ ($\text{m}^3/\mu\text{g}$) vs $\log p_L^0$ (Pa) for PAHs over Lake Michigan (a) 7/21/94 (b) 7/24–25/94 (c) 7/27–28/94 (d) all samples ($n = 17$).

samples collected during February, 1988 (-0.69 and -4.61 , $r^2 = 0.73$). The slope (-0.51) and intercept (-4.28 , $r^2 = 0.57$) for PCBs in Chicago do not compare as well (-0.73 and -5.18 , $r^2 = 0.69$). However, this study analyzed many more congeners than the Cotham and Bidleman study (16) (80 for this study vs 34 for Cotham and Bidleman).

Several factors can account for slopes > -1 , including (1) increasing atmospheric concentration during sampling (4); (2) decreasing temperature during sampling episodes (4); (3) nonequilibrium (4); (4) nonexchangeability (32), (5) varying differences between enthalpies of desorption and volatilization (4); (6) varying number of available adsorption sites (4); and (7) varying activity coefficients in organic matter within a compound class (2). The sampling protocol of two, 12 h samples per day, one during the day and one at night, minimized the effect of changing temperature and atmo-

spheric concentration during sampling. The temperature rarely varied by more than 4°C over any given sampling period. There were also periods of increasing and decreasing temperature, indicating that decreasing temperature cannot account for the shallow slopes. Successive samples occasionally yielded significantly different concentrations (17). While it is impossible to know definitively the change in concentration during the sampling period, samples of low concentration were followed by high concentration samples just as often as the reverse, suggesting that there could have been both increasing as well as decreasing concentrations during individual sampling periods.

Nonexchangeability can occur for PAHs because they are formed in combustion processes. The more volatile species may become trapped inside particles during formation resulting in elevated K_p values (32). This is not likely for

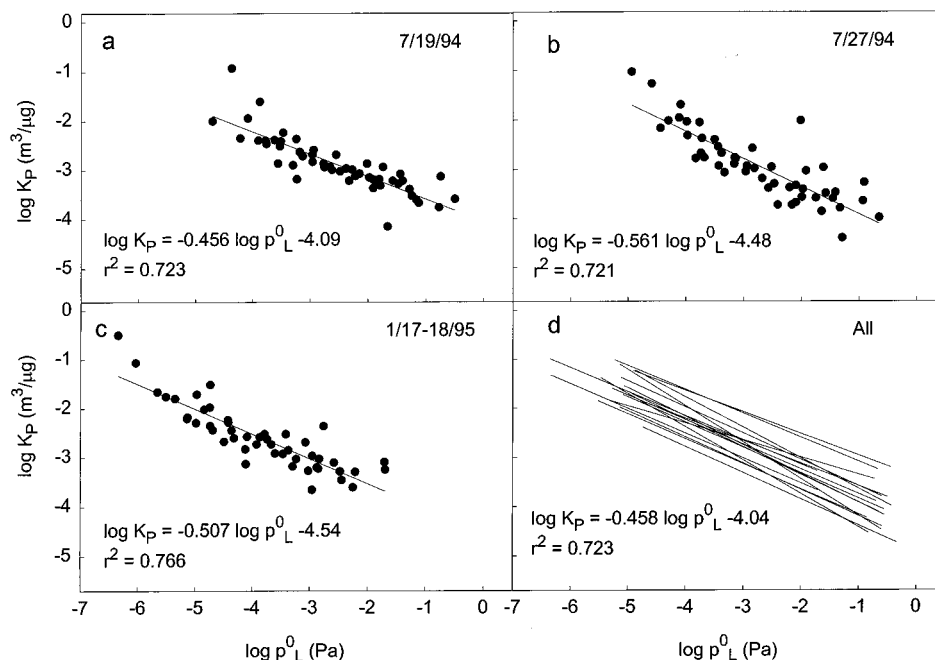


FIGURE 3. $\log K_p$ ($\text{m}^3/\mu\text{g}$) vs $\log p_L^0$ (Pa) for PCBs in Chicago (a) 7/19/94 (b) 7/27/94 (c) 1/17/18/95 (d) all samples ($n = 17$).

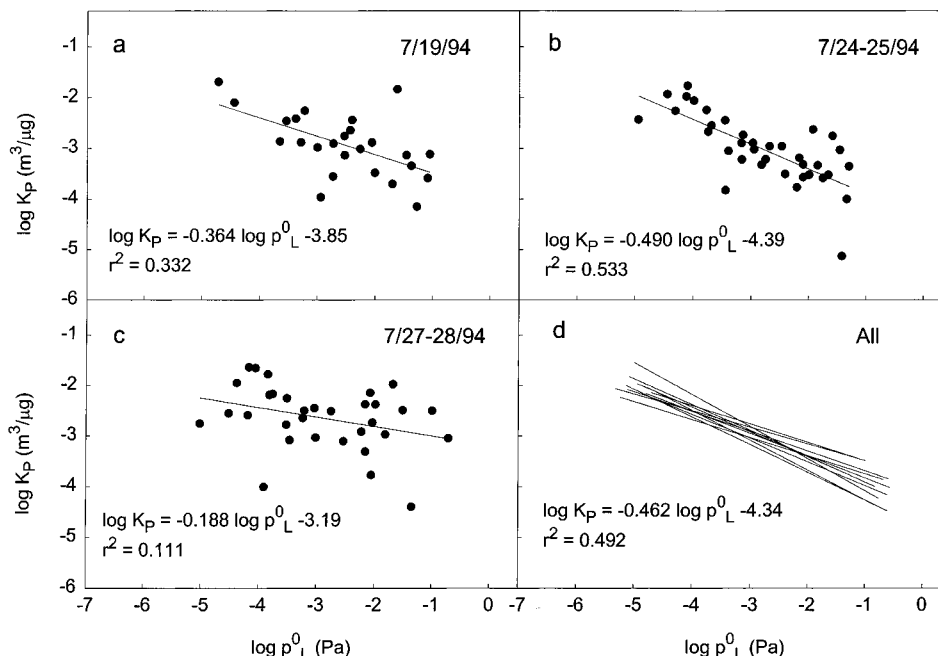


FIGURE 4. $\log K_p$ ($\text{m}^3/\mu\text{g}$) vs $\log p_L^0$ (Pa) for PCBs over Lake Michigan (a) 7/19/94 (b) 7/24-25/94 (c) 7/27-28/94 (d) all samples ($n = 11$).

PCBs which are emitted into the atmosphere primarily as gases volatilized from areas where they have been used, stored, spilled, or atmospherically deposited. It is not possible to determine what, if any, PAHs are nonexchangeable and, therefore, may be a possible reason for the shallow slopes observed for PAHs, but not PCBs.

The issue of nonequilibrium represents a kinetic problem in which the lower molecular weight PCBs and PAHs have higher diffusivities and, therefore, approach equilibrium faster than the higher molecular weight species resulting in data that have a steep slope for PCBs and PAHs with higher vapor pressures and a decreasing slope as vapor pressure decreases (4). In this case, the data are not truly linear. Our data do not exhibit a decreasing slope with decreasing vapor pressure, and a straight line best represents the correlation between partitioning and subcooled liquid vapor pressure.

Another indication that kinetics are not affecting the slope is found when comparing regressions of samples representing air masses that originate in the urban/industrial complex, and ones that represent continental background. Cotham and Bidleman (16) suggested that PAHs from Green Bay, WI, were much closer to equilibrium than Chicago because they represented aged aerosols that traveled further from their source(s), and hence had more time to reach equilibrium. Several samples were taken over Lake Michigan when the wind was from the north, bringing an aged aerosol representative of the continental background signal (17). PAH and PCB data from these samples provide slopes that are among the shallowest observed (-0.53 to -0.70 and -0.56 to -0.16 , respectively). The slopes for the PAH data compare well with values from Lake Superior from McVeety and Hites (-0.59) (14) and Baker and Eisenreich (-0.61) (15) as

TABLE 2. Regression Statistics from Figure 5^a

sample	slope	lower 95%	upper 95%	intercept	lower 95%	upper 95%	r ²
PAH, Chicago	-0.734	-0.851	-0.617	-4.02	-4.40	-3.65	0.969
PAH, Lake Michigan	-0.811	-0.987	-0.636	-4.25	-4.83	-3.67	0.955
PCB, Chicago	-0.517	-0.610	-0.423	-4.35	-4.63	-4.08	0.699
PCB, Lake Michigan	-0.634	-0.754	-0.514	-4.72	-5.06	-4.37	0.699

^a $\log K_p = m \log p_L^0 + b$.

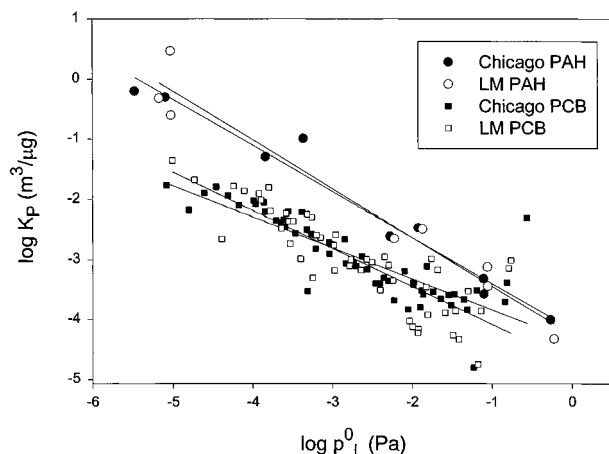


FIGURE 5. Plot of $\log K_p$ ($\text{m}^3/\mu\text{g}$) vs $\log p_L^0$ (Pa) for July 22 night time sample at IIT and Lake Michigan representing the same air mass sampled twice.

calculated in Pankow and Bidleman (4) for the same PAHs. If the aged aerosol of the continental background is in fact at equilibrium, then the necessity of a slope of -1 does not apply universally to all systems. Chicago also received wind from the north during this same time period, but air samples collected represent relatively clean particles entering a contaminated area, and the assumption of long residence time for both gas and particle phases is not valid.

Another approach to addressing the question of non-equilibrium is to observe any changes in the slope of $\log K_p$ vs $\log p_L^0$ as the air mass moves from the urban to adjacent coastal atmosphere. For the overnight sample of July 22 in particular, the wind direction as measured at the ship was consistently from the urban sampling site. The wind speed during this sample was 2.4 m/s, and the distance of 30 km gives a transport time of approximately 3.4 h between sites. Studies of relative times to equilibrium suggest that the kinetics of gas-particle sorption are fast, and a few hours is sufficient for the SOCs to approach equilibrium (33, 34). However, the plot of $\log K_p$ vs $\log p_L^0$ shows no significant change in partitioning between the Chicago and Lake Michigan samples for either PCBs or PAHs (Figure 5), despite the fact that the concentrations over Lake Michigan are about one-third those measured in Chicago (17). The Lake Michigan sample has a much lower concentration due to dispersion and deposition to the lake surface en route. Deposition will preferentially remove the particle phase from the atmosphere. The data support the conclusion that PAHs and PCBs are able to re-equilibrate to compensate for any alteration of the particle composition. All slopes are significantly different from -1 (Table 2). This suggests that both samples are at equilibrium and that other factors exert a dominant influence on the slopes of these plots. The values of K_p for the PAHs are much higher than for PCBs of similar vapor pressures. One explanation for this difference could be the presence of nonexchangeable PAHs, compounds "trapped" on the interior of particles.

If the PCBs and PAHs are at equilibrium and the shallow slopes cannot be attributed to changing concentrations and

temperatures, then the deviation from -1 must result from variations within each compound class for either one or a combination of the final three factors mentioned above, namely the variability in the number of adsorption sites, differences between enthalpies of desorption and volatilization and activity coefficients in organic matter.

Any change in the number of available adsorption sites within a compound class would have to be a result of steric hindrance. Many types of material exhibit surface irregularities on the molecular scale, and it is suggested that this may affect the surface chemistry of these materials (35). If indeed atmospheric particles exhibit these irregularities, the possibility that the number of available adsorption sites are not constant over a compound class may exist. Some of the larger molecules could perhaps be sterically excluded from some sites. If this were the case, however, one would expect the PAHs to be affected to a greater degree than PCBs because of their broader range in molecular sizes. The slopes for PCBs are in fact shallower than for PAHs, contradicting this possibility.

Activity coefficients in organic matter are also expected to remain constant for PAHs and PCBs based on studies of octanol-air partitioning (6) and liquid-like organic matter from cigarette smoke (36). Assuming that these materials are appropriate surrogates for atmospheric organic matter, the slope should be near -1 for absorption dominated partitioning. A compound's absorption into octanol and liquid-like organic matter may not differ from the pure liquid phase of that compound, unlike more solid organic matter that may be present on atmospheric particles like plant waxes. Until characterization of the organic matter associated with atmospheric particulate matter can be accomplished, this remains a question.

As mentioned earlier the energy difference in ($Q_l - Q_v$) among PAHs and PCBs should remain constant (3), but this conclusion was drawn from data that resulted in slopes near -1 . It is not clear that this difference must remain constant for all atmospheric particles under all conditions (4). Whether adsorption or absorption dominates the sorption process, it is clear that the energy terms (enthalpies/activity coefficients) are the major factors contributing to the shallow slopes of $\log K_p$ vs $\log p_L^0$ for PAHs and PCBs in Chicago and over Lake Michigan. The variability in the energy terms represent sorbent properties, and differences in the chemical composition of atmospheric particles would affect these terms. In order to investigate this further it will be necessary to determine the chemical composition of the atmospheric particles to determine if different types of particulate matter result in different partitioning behavior. Knowledge of the chemical compositions may also aid in determining the dominant sorption mechanism.

Acknowledgments

We would like to thank Captain Ronald Ingram and the crew of the *RV Lake Guardian* for their assistance in ship-board measurements, and Clyde Sweet at the Illinois State Water Survey for the TSP data. The AEOLUS project was funded by the United States Environmental Protection Agency (Grant EPA CR 822046-01-0; Alan Hoffman, NERL/RTP, Project

Officer). We especially acknowledge the assistance of Jacki Bode and Angela Bandemehr of the Great Lakes National Program Office (U.S. EPA) for their support and assistance.

Supporting Information Available

Four tables (10 pages) will appear following these pages in the microfilm edition of this volume of the journal. Photocopies of the Supporting Information from this paper or microfiche (105 × 148 mm, 24× reduction, negatives) may be obtained from Microforms Office, American Chemical Society, 1155 16th St. NW, Washington, DC 20036. Full bibliographic citation (journal, title of article, names of authors, inclusive pagination, volume number, and issue number) and prepayment, checked or money order for \$22.50 for photocopy (\$24.50 foreign) or \$12.00 for microfiche (\$13.00 foreign), are required. Canadian residents should add 7% GST. Supporting Information is also available via the World Wide Web at URL <http://www.chemcenter.org>. Users should select Electronic Publications and then Environmental Science and Technology under Electronic Editions. Detailed instructions for using this service, along with a description of the file formats, are available at this site. To download the Supporting Information, enter the journal subscription number from your mailing label. For additional information on electronic access, send electronic mail to si-help@acs.org or phone (202)872-6333.

Literature Cited

- (1) Pankow, J. F. *Atmos. Environ.* **1987**, *21*, 2275–2283.
- (2) Pankow, J. F. *Atmos. Environ.* **1994**, *28*, 185–188.
- (3) Pankow, J. F. *Atmos. Environ.* **1991**, *25A*, 2229–2239.
- (4) Pankow, J. F.; Bidleman, T. F. *Atmos. Environ.* **1992**, *26A*, 1071–1080.
- (5) Harner, T.; Mackay, D. *Environ. Sci. Technol.* **1995**, *29*, 1599–1606.
- (6) Harner, T.; Bidleman, T. F. *J. Chem. Eng. Data* **1996**, *41*, 895–899.
- (7) Harner, T.; Bidleman, T. F. Submitted for publication.
- (8) Foreman, W. T.; Bidleman, T. F. *Environ. Sci. Technol.* **1987**, *21*, 869–875.
- (9) Ligocki, M. P.; Pankow, J. F. *Environ. Sci. Technol.* **1989**, *23*, 75–83.
- (10) Cotham, W. E.; Bidleman, T. F. *Environ. Sci. Technol.* **1992**, *26*, 469–478.
- (11) Gustafson, K. E.; Dickhut, R. M. *Environ. Sci. Technol.* **1997**, *31*, 140–147.
- (12) Falconer, R. L.; Bidleman, T. F.; Cotham, W. E. *Environ. Sci. Technol.* **1995**, *29*, 1666–1673.
- (13) Foreman, W. T.; Bidleman, T. F. *Atmos. Environ.* **1990**, *24A*, 2405–2416.
- (14) McVeety, B. D.; Hites, R. A. *Atmos. Environ.* **1988**, *22*, 511–536.
- (15) Baker, J. E.; Eisenreich, S. J. *Environ. Sci. Technol.* **1990**, *24*, 342–352.
- (16) Cotham, W. E.; Bidleman, T. F. *Environ. Sci. Technol.* **1995**, *29*, 2782–2789.
- (17) Simcik, M. F.; Zhang, H.; Eisenreich, S. J.; Franz, T. P. *Environ. Sci. Technol.* **1997**, *31*, 2141–2147.
- (18) McDow, S. R.; Huntzicker, J. J. *Atmos. Environ.* **1990**, *24A*, 2563–2572.
- (19) Hart, K. M.; Isabelle, L. M.; Pankow, J. F. *Environ. Sci. Technol.* **1992**, *26*, 1048–1052.
- (20) Hart, K. M.; Pankow, J. F. *Environ. Sci. Technol.* **1994**, *28*, 655–661.
- (21) Coutant, R. W.; Brown, L.; Chuang, J. C.; Riggan, R. M.; Lewis, R. G. *Atmos. Environ.* **1988**, *22*, 403–409.
- (22) Katz, M.; Chan, C. *Environ. Sci. Technol.* **1980**, *14*, 838–843.
- (23) VanVaeck, L.; VanCauwengergh, K.; Janssens, J. *Atmos. Environ.* **1984**, *18*, 417–430.
- (24) Zhang, X.; McMurry, P. H. *Environ. Sci. Technol.* **1991**, *25*, 456–459.
- (25) Chuang, J. C.; Hannan, S. W.; Wilson, N. K. *Environ. Sci. Technol.* **1987**, *21*, 798–804.
- (26) Keller, C.; Bidleman, T. F. *Atmos. Environ.* **1984**, *18*, 837–845.
- (27) Ligocki, M. P.; Pankow, J. F. *Anal. Chem.* **1985**, *57*, 1138–1144.
- (28) Liu, S.-P. Doctor of Philosophy Thesis, University of Minnesota, Minneapolis, 1994, 210 pp.
- (29) Krieger, M. S.; Hites, R. A. *Environ. Sci. Technol.* **1994**, *28*, 1129–1133.
- (30) Kaupp, H.; Umlauf, G. *Atmos. Environ.* **1992**, *26A*, 2259–2267.
- (31) Falconer, R. L.; Bidleman, T. F. *Atmos. Environ.* **1994**, *28*, 547–554.
- (32) Pankow, J. F.; Bidleman, T. F. *Atmos. Environ.* **1991**, *25A*, 2241–2249.
- (33) Rounds, S. A.; Pankow, J. F. *Environ. Sci. Technol.* **1990**, *24*, 1378–1386.
- (34) Kamens, R.; Odum, J.; Fan, Z.-H. *Environ. Sci. Technol.* **1995**, *29*, 43–50.
- (35) Avnir, D.; Farin, D.; Pfeifer, P. *Nature* **1984**, *308*, 261–263.
- (36) Liang, C.; Pankow, J. F. *Environ. Sci. Technol.* **1996**, *30*, 2800–2805.

Received for review June 25, 1997. Revised manuscript received October 8, 1997. Accepted October 22, 1997.*

ES970557N

* Abstract published in *Advance ACS Abstracts*, December 1, 1997.